Roman coloured and opaque glass: a chemical and spectroscopic study

Appl. Phys. A 83, 239–245 (2006)
DOI: 10.1007/s00339-006-3515-2

Applied Physics A
Materials Science & Processing

R. ARLETTI[1,✉]
M.C. DALCONI[2]
S. QUARTIERI[3]
M. TRISCARI[3]
G. VEZZALINI[1]

Roman coloured and opaque glass: a chemical and spectroscopic study

[1] Dipartimento di Scienze della Terra, L. go S. Eufemia, 19, 41100 Modena, Italy
[2] Dipartimento di Scienze della Terra, Via Saragat, 1, 44100 Ferrara, Italy
[3] Dipartimento di Scienze della Terra, Salita Sperone, 31, 98166 Messina S. Agata, Italy

Received: 5 December 2005/Accepted: 12 December 2005
Published online: 21 February 2006 •

ABSTRACT This work reports the results of an archaeometrical investigation of opaque Roman glass and is mainly focussed on the role of configuration and oxidation state of copper on the colour and opacity of red and green opaque finds (mosaic tesserae, game counters, and glass artefacts) from Sicily and Pompeii excavations. The glass fragments were characterised by EMPA, SEM-EDS, TEM, and XRPD analyses and the copper local environment was investigated using X-ray absorption spectroscopy. The analyses of high-resolution Cu-*K* edge XANES and EXAFS spectra suggest that, in red samples, copper is present as monovalent cations coordinated to the oxygen atoms of the glass framework, accompanied by metallic clusters. In green samples all the copper cations are incorporated in the glass matrix.

PACS 61.10.Ht; 61.43.Fs; 61.46.+w

1 Introduction

The colour of glass is determined by the oxidation state and the electronic configuration of the associated metal ions [1, 2]. Regarding red glass, Weyl [3] stated that coloration is always produced by crystals of metallic copper dispersed in the glass matrix, the differences in the final colour being mainly related to the dimensions of the particles (particles < 50 nm lead to transparent red glass called 'copper-ruby' and a particle size around a few hundred nm gives an opaque red glass). Mirti et al. [4], studying fragments of 7th–8th century glass from Cripta Balbi in Rome, found some red opaque samples containing small spherules, smaller than 1-μm across, dispersed in a homogeneous matrix. The energy dispersive spectrometry (EDS) analyses and the X-ray powder diffraction (XRPD) spectra confirmed the presence of metallic copper in the glass. Otherwise, a study performed by Brun et al. [5] on Celtic opaque red glass containing lead revealed the presence of a large number of dendritic crystals of cuprous oxide (Cu_2O), together with a few metallic copper nodules. Thus, red opaque glass can contain metallic copper as well as cuprous oxide. A recent study performed by X-ray absorption spectroscopy (XAS) on the red Satsuma ancient glass and on reproduced (red and colourless) glass samples [6] revealed that the majority of copper was present as monovalent cations coordinated to three or four oxygen atoms in the glass matrix. However, since the reproduced colourless glass also revealed a high level of Cu^{1+}, the authors concluded that monovalent copper ions do not play any role in glass coloration. The red colour of this ancient ruby glass was ascribed to colloidal particles of metallic copper, undetected by XAS. Padovani et al. [7, 8], in a study of red lustre decorations of Italian Renaissance pottery, found that the majority of copper was present as monovalent species, along with a minor level of metallic nano-particles. They concluded that the chromatic effect was determined only by the fraction of metal ions reduced to nano-particles.

As regards green glass, copper generally occurs in its oxidised form (Cu^{2+}), and the ions are present in the glass framework bonded to the oxygen atoms, imparting the distinctive turquoise colour to the glass [9].

It has been largely demonstrated that XAS is a powerful means for obtaining structural information on a specific absorbing element. This technique has the advantage of being nondestructive, element selective, and sensitive to low concentrations and hence represents a suitable tool for cultural heritage studies. In recent years, in fact, X-ray absorption near edge structure (XANES) and X-ray absorption fine structure (EXAFS) techniques have been successfully applied to the study of colour of several ancient glass and lustre samples, providing information on the chemical state of the colouring agents [7, 8, 10, 11]. Since the characterisation of colourants is fundamental for investigating the manufacturing methods of ancient glass, we applied – besides micro-analytical and imaging techniques – the XAS method to study the oxidation state and the coordination of Cu in red, blue, and blue-green samples.

2 Samples

All the analysed glass samples, dated between the I and III century A.D., come from two Sicilian sites (Tusa and Lipari, Italy) [12] and Pompeii [13]. All the samples are coloured and most of them are opaque and represent different typologies of glass item, including mosaic

✉ Fax: +39-059-2055887, E-mail: rarletti@unimore.it

Sample	PM11313-5	PM35117	PM3191A	VL3	BL4	BTS5	RL6	RT7	PM9361A
Provenance	Pompeii	Pompeii	Pompeii	Lipari	Lipari	Tusa	Lipari	Tusa	Pompeii
Age	I cen A.D.	I cen A.D.	I cen A.D.	III cen A.D.	III cen A.D.	III cen A.D.	III cen A.D.	III cen A.D.	I cen A.D.
Colour	O. Blue-green	O. Green	O. Yellow-green	T. Green	T. Blue	O. Blue	O. Red	O. Red	O. Red
SiO_2	69.09	61.52	72.77	60.67	64.22	67.21	61.17	63.04	64.60
TiO_2	0.12	0.17	0.16	0.13	0.13	0.08	0.18	0.18	0.15
Al_2O_3	2.24	2.02	2.32	2.66	2.19	2.46	2.04	3.24	3.50
FeO	0.88	0.98	0.91	0.53	0.60	1.77	1.37	2.71	2.17
MnO	0.38	0.48	0.34	0.11	0.13	0.46	0.40	0.46	0.40
MgO	1.14	1.15	0.79	3.73	3.61	0.49	2.64	1.04	1.08
CaO	6.57	5.90	3.08	9.22	8.35	5.09	8.89	6.63	8.44
Na_2O	18.47	16.45	18.90	16.19	16.33	15.56	14.66	16.49	16.21
K_2O	0.84	1.58	0.54	3.56	3.20	0.74	2.52	1.47	1.45
Sb_2O_5	1.85	2.67	1.35	0.07	0.08	4.99	0.30	0.66	0.28
PbO	0.28	3.11	6.00	0.04	0.25	0.12	2.12	1.81	0.52
CuO	0.85	3.99	0.27	4.25	0.07	0.81	2.63	2.10	1.80
CoO	0.00	0.01	0.00	0.01	0.04	0.48	0.01	0.00	0.00

TABLE 1 Glass chemical analyses obtained by WDS-EMPA for opaque (O.) and transparent (T.) samples, respectively

tesserae, game counters, vessels, and other artefacts (see Table 1). The attention was focussed on green, blue-green, and red samples, i.e. on samples containing high copper levels.

3 Experiment

3.1 *Electron microprobe analyses*

Before collecting XAS spectra, the samples were extensively characterised from the chemical and mineralogical points of view. The quantitative chemical analyses of the glass were performed using an ARL-SEMQ microprobe equipped with four scanning wavelength dispersive spectrometers (WDS-EMPA) sited at the Earth Science Department of the University of Modena e Reggio Emilia. The elements analysed were: Si, Ti, Al, Mn, Mg, Fe, Ca, K, Na, Co, Sb, Cu, and Pb. A series of certified natural minerals were employed as standards. The analyses were performed operating at 15 kV and 20 nA using counting times of 5 s–10 s–5 s on background–peak–background, respectively. Due to the known loss of light elements under the electron beam [14], a defocussed beam (30 μm) was used. The results were processed for matrix effects using the program Probe [15] with the Armstrong PHI absorption correction and the oxide percentages were computed.

3.2 *SEM-EDS and TEM analyses*

A number of backscattered images were collected on each sample with a Philips XL40 scanning electron microscope (SEM) – sited at the Centro Interdipartimentale Grandi Strumenti of the University of Modena e Reggio Emilia – to evaluate the presence of high atomic number phases dispersed as opacifiers in the glass matrix. Their qualitative chemical analyses were obtained with an EDS spectrometer (Oxford SATW). The analyses were performed on the polished samples using an acceleration voltage of 25 kV. Transmission electron microscopy (TEM) images were obtained on a JEOL 2010 TEM – sited at the Centro Grandi Strumenti of the University of Modena and Reggio Emilia – operating at 200 kV. The microscope was equipped with a slow-scan camera (Gatan 694) for collecting images and with an INCA 100 Oxford EDS system which allowed the obtaining of qualitative chemical compositions. The glass samples were ground in an agate mortar and then deposited (as a suspension in isopropyl alcohol) on a carbon film Ni grid.

3.3 *XRPD analysis*

X-ray diffraction (XRD) experiments were performed to identify the crystalline phases dispersed in the glass matrix. The analyses were carried out with a Philips PW1729 diffractometer with Bragg–Brentano geometry $\theta/2\theta$ and Cu K_α radiation, using a zero background quartz holder. The spectra were collected from 5 to 80° 2θ using a 0.02θ step and counting time of 4 s for each step.

3.4 *XAS experiments*

Cu-*K*-edge XANES spectra were collected directly on glass fragments in fluorescence mode at the GILDA-CRG beamline (ESRF, Grenoble, France). A dynamically and sagittally focussing monochromator with Si(311) crystals [16] was used. Reference spectra were collected in transmission mode on a Cu foil and on powdered CuO and Cu_2O deposited on millipore membranes. Energy calibrations were achieved using the spectra of copper foil as references and the position of the first inflection point was taken at 8989.7 eV. All the XANES spectra were collected at room temperature. EXAFS measurements were performed at 77 K in fluorescence mode on selected red RT7 and green PM35117 samples and on the reference compounds (metallic Cu, Cu_2O, CuO). The EXAFS signals were extracted from the experimental absorption spectra and analysed using the interactive program IFEFFIT [17] with the support of the graphical utilities ATHENA and ARTEMIS [18]. The theoretical EXAFS signals were calculated using the FEFF8 code [19]. The results of the fitting procedure, performed up to the second shell around the absorbing atom, are reported in Table 3. A Fourier transform (FT) was performed in the interval $k = 3.6$–11.0 Å^{-1} with a k^2-weight for the red sample and in the interval $k = 3$–10 Å^{-1} with a k^1-weight for the green sample. The back-FT was computed in the intervals 1–2.8 Å and 0.9–2.1 Å, for the red and green samples, respectively. The multi-electron amplitude reduction factor S_0^2 in the EXAFS formula was fixed to the value obtained from the CuO EXAFS spectrum ($S_0^2 = 0.8$).

4 Results and discussion

4.1 *Chemical composition*

The chemical analyses of the major elements (Table 1) reveal that most of the samples are silica-soda-lime glass, typical of the Roman age, produced with calcareous siliceous sand as vitrifying material and natron as flux [2, 20–22]. Only the three samples coming from Lipari (VL3, BL4, and RL6) show higher levels of MgO and K_2O, suggesting the use of a different source of flux. In fact, levels of these two oxides above 2.5% have usually been found in plant-ash-based glass [23] produced with an organic sodium-rich flux (usually deriving from marine plants) also containing K and Mg.

The differences in the minor elements (in particular in Cu, Co, Sb, and Pb) are mainly related to the colour and opacity of the samples. The highest values of PbO, along with quite high values of Sb_2O_5, are present in opaque green and yellow-green samples. Furthermore, high levels of antimony are also present in blue and blue-green opaque glass. All the red samples show significant copper contents and Cu is also present in all the green glass, even if only samples PM35117 and VL3 are Cu-rich. Cobalt is present only in the blue samples, associated with low amounts of copper, whereas iron is present in all the samples analysed, the highest concentrations always in red glass.

4.2 *SEM-EDS and XRPD results: opacifing agents*

SEM-EDS and XRPD analyses were performed with the aim of identifying the opacifying agents employed in the production of these opaque Roman glass artefacts. All the images collected by back scattered electrons (BSE) on the opaque samples revealed the presence of small particles with mean atomic numbers higher than the matrix. In particular, in yellow-green and green samples, aggregates of particles containing lead and antimony were detected. Furthermore, the XRPD analyses revealed the presence of $Pb_2Sb_2O_7$ crystals in these samples. The colour exhibited by the yellow-green sample is probably due to the combined presence of the yellow lead antimonate as opacifier and of copper and iron as colouring agents. In blue and blue-green opaque samples, the BSE images, coupled with the EDS spectra, demonstrated the presence of small crystals of calcium antimonate. This result is in agreement with the XRPD pattern, which shows several peaks characteristic of the $CaSb_2O_6$ phase. In this case, the presence of cobalt – even if in low amounts – assures the blue colour of these samples.

Regarding the opaque red glass, the XRPD pattern shows, along with a strong background due to the glassy matrix, two very weak peaks corresponding to the (111) and (220) reflections of Cu^0. BSE images evidence rare large (a few microns) spherules of copper sulphide accompanied by other very small particles well dispersed in the matrix (Fig. 1). These small particles, certainly containing copper as revealed by the EDS analysis, were also evidenced by TEM images (Fig. 2). This last technique also allowed us to determine the size distribution of the clusters, which is peaked around 40–50 nm (Fig. 3). However, from these data it was not possible to understand if copper was also present in the glass matrix as cations. Hence,

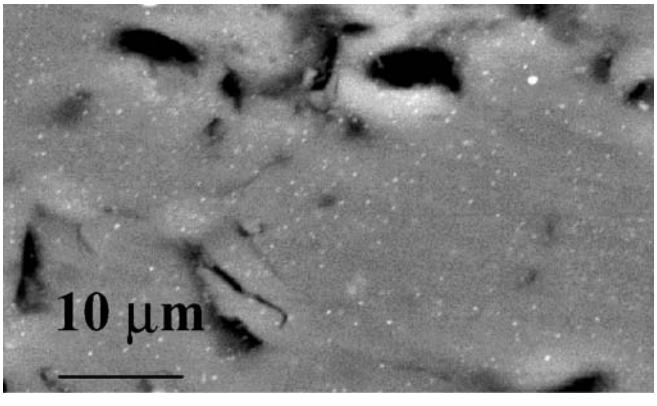

FIGURE 1 BSE image of the red sample RT7

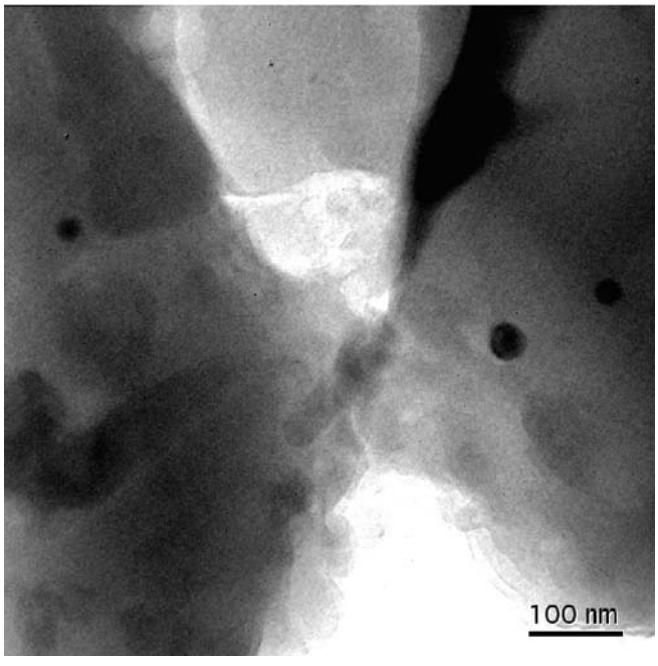

FIGURE 2 Bright-field TEM image of the red sample RT7

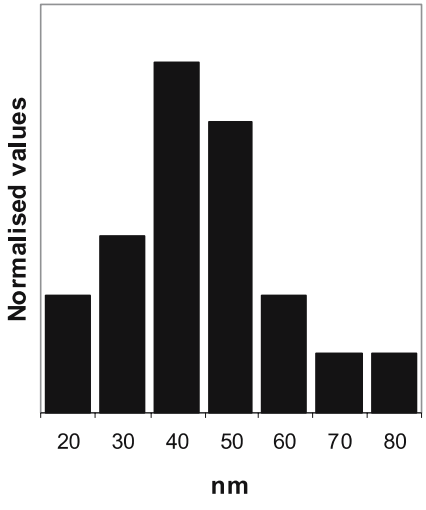

FIGURE 3 Histogram reporting the size distribution of the copper clusters determined by TEM

a XAS study was performed to define the oxidation state and the local environment of copper in these samples.

4.3 *XAS results*

Figure 4 reports the XANES spectra of the reference compounds and of selected samples. Table 2 reports the energy positions of the spectral features.

The analysis of the XANES spectra of the three standard compounds shows that there is a shift of the absorption edge towards high energy with increasing oxidation state: a shift of 0.9 eV is observed between the edges of Cu^0 and Cu_2O and one of 3.7 eV between Cu_2O and CuO. In general, all the features of the CuO spectrum are strongly shifted towards higher energy when compared with those of the other reference compounds. Moreover, the CuO spectrum exhibits a very weak absorption peak at about 8978 eV (Fig. 4), attributed to the dipole-forbidden $1s \rightarrow 3d$ transition, which is absent in the other copper compounds.

The edge peak at about 8903 eV (labelled e in Fig. 4), due to the dipole-allowed transition $1s \rightarrow 4p$, is extremely intense in all the glass here studied. A similar very intense edge peak was observed by Kuroda et al. [24] in a copper-ion-exchanged ZSM-5 zeolite. The energy positions of the XANES features are compatible with Cu^{1+}, and the high intensity of the $1s \rightarrow 4p$ peak was ascribed by the authors to the coordination geometry of copper, which was found to be bonded to three framework oxygen atoms at a distance of about 1.9 Å. These data will support our conclusions, reported below, that is, that in our samples Cu cations are mainly monovalent and dispersed in the glass matrix via coordination with the oxygen atoms.

4.3.1 Red glass. The positions of edge, shoulder, and edge crest of the red sample lie at 8983.6, 8992.2, and 8995.6 eV, respectively (Table 2), and match better with the positions found in Cu_2O rather than those of metallic copper. In fact, for Cu^0 these three features are shifted by about 2 eV towards lower energy. However, two further features found in the sample spectrum above the edge (labelled a and d in Table 2 and Fig. 4) do not appear in the Cu_2O spectrum, while they are present in that of metallic copper. These two features are also present in the Cu-K-edge XANES spectrum of a red mosaic glass from the Dome of Hagia Sophia (Istanbul) studied by Nakai et al. [10], and were attributed by the authors to the presence of metallic copper. Hence, the XANES data for the red sample studied here suggest the presence of monovalent copper accompanied by metallic copper, this last already evidenced by TEM and XRD.

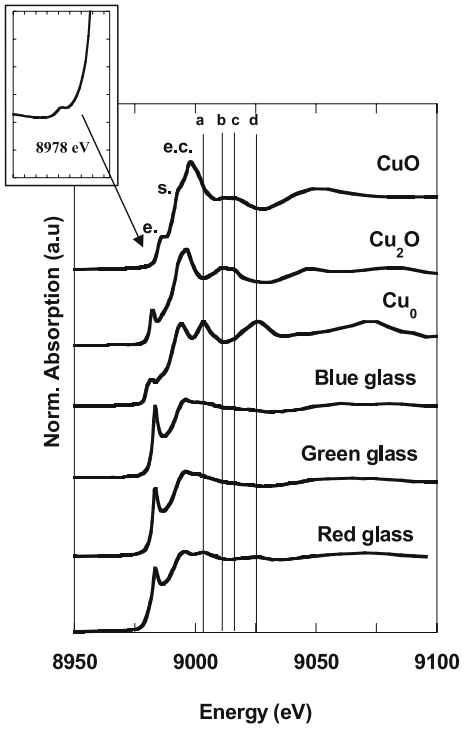

FIGURE 4 Cu-K-edge XANES spectra for blue, green, and red glass samples, compared with those of reference compounds

Further structural information was obtained by EXAFS analysis. The EXAFS signal of sample RT7 and its Fourier transform are compared with those of the standard metallic copper in Fig. 5a and b, respectively. All the features of the reference foil are also present in the sample signals, but, as ev-

Sample	Colour	Edge (e.)	1° shoulder (s.)	Edge crest (e.c.)	a	b	c	d
PM11313-5	Green	8983.3	8992.2	8996.3				
PM35117	Dark green	8983.3	8992.5	8996.2				
PM3191A	Yellow-green	8983.4	8992.1	8996.2				
VL3	Green	8983.3	8992.7	8996.1				
BL4	Dark blue	8983.3	8992.7	8996.1				
BTS5	Dark blue	8983.3	8992.7	8996.2				
RL6	Red	8383.1	8992.4	8995.6	9003.3			9025.5
RT7	Red	8983.3	8992.4	8995.6	9003.3			9025.6
PM9361A	Red	8983.6	8992.2	8995.6	9003.2			9026.9
Standards		Edge	1° shoulder	Edge crest	Feat a	Feat b	Feat c	Feat d
CuO		8986.2	8993.0	8998.5	–	–	9015.8	–
Cu_2O		8982.5	8991.7	8995.9	–	9011.4	9015.8	–
Cu		8981.6	8989.7	8994.1	9003.1	–	–	9025.3

TABLE 2 Cu-K-edge feature positions (eV) for the glass samples and the reference compounds. The labels e., s., e.c., a, b, c, d refer to Fig. 1

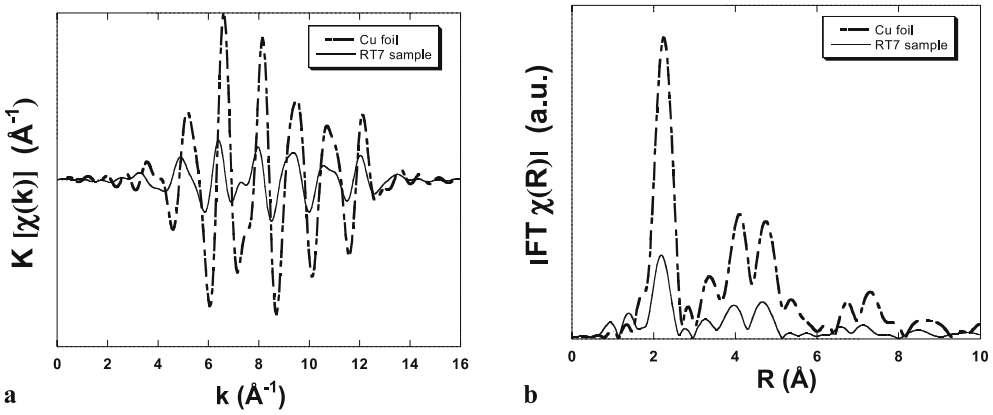

FIGURE 5 Comparison between the moduli of Cu-K-edge EXAFS signals (**a**) and Fourier transforms (**b**) of the red sample RT7 and Cu foil

TABLE 3 Results of EXAFS analysis for red (RT7) and green (PM35117) glass. R, N, σ^2 indicate interatomic distance, coordination number, and Debye–Waller factor, respectively. The structural parameters of the reference compounds are from the Crystallographic Information File

	Cu−O			Cu−Cu		
	R (Å)	N	σ^2 (10^{-4} Å^2)	R (Å)	N	σ^2 (10^{-4} Å^2)
RT7	1.81 ± 0.02	1.51 ± 0.6	30 ± 10	2.54 ± 0.02	11.9 ± 1.2	19 ± 10
				3.59 ± 0.02	5.4 ± 1.9	19 ± 10
				4.39 ± 0.02	22.0 ± 4.4	19 ± 10
PM35117	1.90 ± 0.02	1.80 ± 0.7	38 ± 64			
CuO	1.95	2		2.90	4	
	1.96	2		3.08	4	
Cu_2O	1.85	2		3.02	12	
Cu met	–	–		2.55	12	
				3.61	6	
				4.42	24	

idenced by the reduced intensity, the amount of Cu^0 in RT7 must be rather low. To quantitatively estimate the copper speciation, we have performed a first EXAFS fit including both monovalent and metallic copper phases, with fixed coordination numbers (CN) – from cuprite and metallic copper bulk, respectively – and refining the relative percentages of the two phases and their structural parameters. The use of the CNs of bulk Cu^0 (12, 6, and 24 for the first three shells, respectively) in the EXAFS analysis of the metallic phase present in our sample was suggested by the large dimensions of the clusters, as deduced by the TEM investigation [25]. From this first analysis we estimated the presence of about 25% of Cu^0 and 75% of Cu^+. Adopting these percentages, we performed a second EXAFS multi-shell fit allowing the coordination numbers of the two phases to vary. The results are reported in Table 3 and in Fig. 6a and b, which show the k^2-weighted Fourier transform moduli and the result of the multi-shell fitting procedure of the EXAFS signal collected on sample RT7.

As shown in Table 3, the copper–copper bond distances are in strict agreement with those of metallic copper bulk, coherently with the large dimensions of the clusters dispersed in the glass. Concerning monovalent copper, it is coordinated to oxygen atoms at 1.81 Å, which is in excellent agreement with the Cu−O interatomic distance determined by Padovani et al. [7, 8] for Italian Renaissance pottery and by Nakai et al. for Satsuma copper-ruby glass [6]. These authors suggest that Cu^+ is incorporated in the glass matrix. The bond distance and the CN (1.5 ± 0.6) estimated for Cu^+ in RT7 are also com-

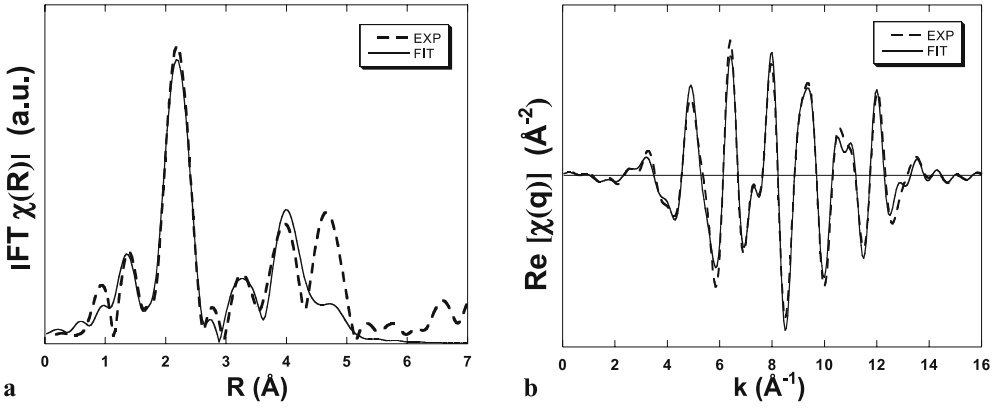

FIGURE 6 Cu-K-edge moduli of Fourier transform (**a**) and best fit (**b**) for the red sample RT7. Transformation was performed in the interval $k = 3.6$–13.0 Å^{-1} with a k^2-weight

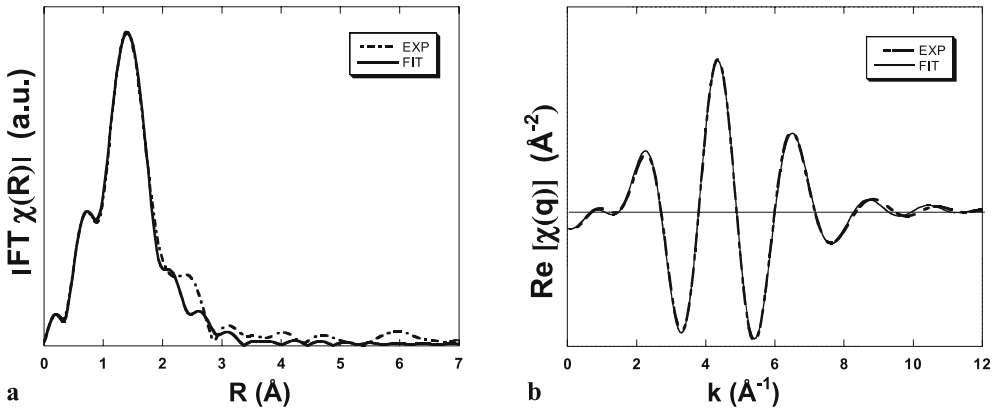

FIGURE 7 Cu-K edge moduli of Fourier transform (**a**) and best fit (**b**) for the green sample PM35117. Transformation was performed in the interval $k = 3$–$10\,\text{Å}^{-1}$ with a k^1-weight

patible with the structure of cuprite. However, since we did not find any evidence of cuprite peaks in the X-ray diffraction pattern collected on this sample, we suggest that monovalent copper is incorporated into the glass framework.

4.3.2 Green and blue glass. All the XANES spectra collected on green and blue samples (opaque and transparent) show the same features in the same energy positions, in particular an absorption edge at 8983.3 eV and a shoulder at 8992.5 eV, followed by an edge crest around 8996 eV. The spectra profiles, rather similar to that obtained for Cu_2O, show the dominating presence of the dipole-allowed transition $1s \rightarrow 4p$ at 8982.5 eV, which is, however, shifted by 0.8 eV towards higher energy with respect to cuprite. The position of the edge crest of all the samples fits with that exhibited by Cu_2O, even if in the samples (especially in the blue ones) this feature is much broader. In general, the spectra of our samples show very different features from those of CuO; in particular, the weak pre-edge peak at 8978 eV is absent. These observations suggest that the dominant species in all these glass samples is monovalent copper dispersed in the glass alumino-silicatic matrix, possibly accompanied by a minor presence of divalent copper. This last species, associated with iron, should be the cause of the green colour of the glass.

The Fourier transform of the green sample PM35117, reported in Fig. 7a, shows the presence of only one major peak, which, on the basis of its position, can be attributed to Cu−O bonds. For a more detailed investigation of number and bond distances of the first-neighbour oxygen atoms, the inverse FT of the first shell was performed (Fig. 7b). The structural parameters obtained after the fitting are summarised in Table 3. The fit proves the presence of about two neighbouring oxygen atoms at 1.90 Å. This distance, completely in agreement with that found in an EXAFS study of implanted copper ions in silica glass [26], is intermediate between that of Cu^{1+} in Cu_2O (1.84 Å) and Cu^{2+} in CuO ($\sim$ 1.95 Å) and is compatible with copper cations coordinated to oxygen atoms of the glass matrix. The relatively low coordination number obtained by our EXAFS analysis could be ascribed to disorder effects typical of the glass structure [6, 27, 28]. It is worth noting that also in this green sample XRPD did not evidence the presence of cuprite.

Finally, based on the well-known colouring efficiency of cobalt (which is able to confer the typical deep-blue colour even when present in a few ppm), it can be argued that blue glass owe their colour to the presence of this element, which, in our samples, is present in concentration levels ranging from a few hundreds to a few thousands of ppm (see Table 1).

5 Conclusions

The results obtained for red glass samples clearly indicate the presence of monovalent copper cations incorporated in the glass matrix, accompanied by Cu nano-clusters. These conclusions are congruent with the red colour and the opaque aspect of the samples and are in agreement with the results reported in the literature for other studies of glass and lustre. In particular, the agreement with the results obtained by Padovani et al. [7, 8] on Renaissance lustre is remarkable, suggesting possible analogies in the two production techniques. The glass composition and the melting conditions are the parameters that control the metal oxidation state. To obtain metallic copper, strong reducing conditions are needed; Ahmed and Ashour [29] succeeded in producing opaque red glass containing metallic copper by adding iron to the final batch, since this element should displace the redox equilibrium of copper to the reduced state. This is in agreement with the results reported in Table 1, which show that all the red samples contain high levels of Fe. However, this hypothesis will be further verified by synthesising glass with different Cu and Fe contents and under different oxidation atmospheres.

As regards the green and blue-green samples, we found that copper is mainly present as Cu^{1+} incorporated in the glass matrix. Minor quantities of divalent copper could be responsible, together with iron, for the colour of the green samples, whereas the intense blue colour of the blue glass is certainly due to the presence of a few hundred ppm of cobalt.

ACKNOWLEDGEMENTS The authors are indebted to Dr. M.A. Mastelloni (Museo Regionale di Messina, Italy) and Dr. A.M. Ciarallo (Laboratorio Ricerche Applicate, Sovrintendenza Archeologica di Pompei) for providing the mosaic tesserae from Sicily and the game counters from Pompeii, respectively, to Dr. Simona Bigi for the help during TEM analyses, to two anonymous referees for the constructive reviewing of the manuscript, and to Eric Dooryhee for his editorial efforts. Financial support was provided by the Italian MIUR (COFIN2002 'Geo-crystal-chemistry of trace elements' to S.Q. and M.T. and COFIN 2004 'Scienza dei materiali antichi derivati da geomateriali: trasferire le conoscenze di base delle geoscienze allo studio di vetri e metalli' to R.A. and G.V.) and by Istituto Nazionale per la Fisica della Materia. GILDA beamline staff (ESRF, Grenoble) are acknowledged for the assistance during the XAS experiments.

REFERENCES

1 R.H. Doremus, *Glass Science*, 2nd edn. (Wiley, New York, 1994)
2 J. Henderson, Oxford J. Anthropol. **4**, 267 (1985)
3 W.A. Weyl, *Coloured Glass* (Corning, New York, 1953)
4 P. Mirti, P. Davit, M. Gulmini, Anal. Bioanal. Chem. **372**, 221 (2002)
5 N. Brun, L. Mazerolles, M. Pernot, J. Mater. Sci. Lett. **10**, 1418 (1991)
6 I. Nakai, C. Numako, H. Hosono, K. Yamasaky, J. Am. Ceram. Soc. **82**, 85 (1999)
7 S. Padovani, C. Sada, P. Mazzoldi, B. Brunetti, I. Borgia, A. Giulivi, S. Sgamellotti, F. D'Acapito, G. Battaglin, J. Appl. Phys. **93**, 158 (2003)
8 S. Padovani, I. Borgia, B. Brunetti, A. Sgamellotti, A. Giulivi, F. D'Acapito, P. Mazzoldi, C. Sada, G. Battaglin, Appl. Phys. A **79**, 223 (2004)
9 R.H. Brill, in *Glass and Glassmaking in Ancient Mesopotamia*, ed. by A.L. Oppenheim, R.H. Brill, D. Barag, A. von Saldern (The Corning Museum of Glass Monogr. **3**) (Corning, New York, 1970), p. 129
10 I. Nakai, M. Matsunaga, M. Adachi, K.I. Hidaka, J. Phys. France IV **2**, 1033 (1997)
11 S. Quartieri, M. Triscari, G. Sabatino, F. Boscherini, A. Sani, Eur. J. Mineral. **14**, 749 (2002)
12 M. Triscari, S. Quartieri, G. Sabatino, G. Vezzalini, R. Arletti, M.A. Mastelloni, Quad. Mus. Reg. Mess. (2005) in press
13 R. Arletti, A. Ciarallo, S. Quartieri, G. Sabatino, G. Vezzalini, in *Geomaterials in Cultural Heritage*, ed. by M. Maggetti, B. Messiga (Spec. Publ. Geol. Soc. Lond. 257 (2006)
14 R. Rinaldi, in *Microscopia Elettronica a Scansione e Microanalisi, Parte II*, ed. by A. Artigliato, U. Valdrè (Lo Scarabeo, Bologna, 1981) p. 245
15 J.J. Donovan, M. Rivers, Microbeam Anal. **66**, 68 (1990)
16 S. Pascarelli, F. Boscherini, F. D'Acapito, J. Hardy, C. Meneghini, S. Mobilio, J. Synchrotron Radiat. **3**, 147 (1996)
17 M. Newville, J. Synchrotron Radiat. **8**, 322 (2001)
18 http://feff.phys.washington.edu/∼ravel/software/exafs/
19 A.L. Ankudinov, B. Ravel, J.J. Rehr, S.D. Conradson, Phys. Rev. B **58**, 7565 (1998)
20 W.E.S. Turner, J. Soc. Glass Technol. **40**, 162 (1956)
21 E.V. Sayre, R.V. Smith, Science **133**, 1824 (1961)
22 M. Verità, in *Le Verre de l'Antiquite Tardive et du Haut Moyen Age, Musee Archeologique Departemental du Val d'Oise*, ed. by D. Foy (AFAV, 1993) (Guiry, 1995) p. 291
23 C. Lilyquist, R.H. Brill, *Studies in Ancient Egyptian Glass* (Metropolitan Museum of Art, New York, 1995)
24 Y. Kuroda, R. Kumashiro, A. Itadani, M. Nagao, H. Kobayashi, Phys. Chem. Chem. Phys. **3**, 1383 (2001)
25 H.G. Fritsche, R.E. Benfield, Z. Phys. D **269**, 15 (1993)
26 K. Fukumi, A. Chayahara, K. Kadono, H. Kageyama, T. Akai, N. Kitamura, M. Makihara, K. Fujii, J. Hayakawa, J. Non-Cryst. Solids **238**, 143 (1998)
27 A. Paul, in *Chemistry of Glasses*, 2nd edn. (Chapman and Hall, London, 1990) p. Ch. 9
28 B.K. Teo, *EXAFS: Basic Principles and Data Analysis* (Springer, Berlin, 1986)
29 A.A. Ahmed, G.M. Ashour, Glass Technol. **22**, 24 (1981)